DOI: 10.1002/anie.200604262

Is Eka-Mercury (Element 112) a Group 12 Metal?**

*Nicola Gaston, Ingo Opahle, Heinz W. Gäggeler, and Peter Schwerdtfeger**

The synthesis of superheavy elements is a challenge for experimental physics that raises fundamental questions about nuclear structure and stability.[1] Considerable progress has already been made with the synthesis of elements with atomic numbers up to $Z = 118$,[2–5] and with the development of real atom-at-a-time chemistry for elements with atomic numbers up to $Z = 108$[6,7] to explore their often anomalous behavior. However, the detection of these elements relies on a good understanding of their chemical and physical properties.

For the transactinide series, which begins with rutherfordium ($Z = 104$), experiments have been performed to correctly place the elements in the Periodic Table and to address the question of whether the Periodic Table is even useful for their categorization. Owing to the very small half-lives of these elements ($t_{1/2} = 78$ (${}^{261}_{104}\mathrm{Rf}$) to 14 s (${}^{269}_{108}\mathrm{Hs}$)), such experiments involve nonstandard procedures and often rely on theoretical predictions for unambiguous interpretation.[8,9]

The latest superheavy element for which atom-at-a-time chemistry is planned is element 112,[10–12] eka-mercury ($t_{1/2} \approx 4$ s for ${}^{283}112$[13]). The chemistry of element 112 is controversial: earlier predictions ranged from mercury-like properties[16,17] to noble-gas-like behavior[8,18,19] resulting from the strong relativistic contraction of the 7s shell. Hence, model studies based on the assumed similarity of element 112 to either the noble gas radon or to the transition metal mercury have been conducted.[10–12,14,15] Predicted data for the elements 112 and 114 were used to correlate their sublimation and adsorption behavior on metal surfaces.[20,21] Such predictions are extremely valuable for the design of sophisticated experimental setups for the chemical investigation of the transactinide elements on a single-atom scale.

The relativistic contraction of the valence s shell is already of fundamental importance for mercury. Relativistic effects lead to a van der Waals interaction between the inert closed 6s shells in the mercury dimer, which is responsible for the distinctive behavior of mercury in comparison to that of zinc or cadmium. In the condensed state, mercury, with a resistivity of $\rho = 5.8\ \mu\Omega\,\mathrm{cm}$ at 77 K, is a much poorer metal than zinc ($\rho = 1.1\ \mu\Omega\,\mathrm{cm}$) or cadmium ($\rho = 1.6\ \mu\Omega\,\mathrm{cm}$),[22] and adopts an uncommon rhombohedral structure.[23] Indeed, it is possible to implicate relativistic effects in the very low melting temperature of the bulk element. However, bulk mercury in the solid state is very different from the condensed noble gases. In the case of element 112, these effects are expected to be further amplified.[24–27] This likelihood leads to the question of whether element 112 is, in fact, metallic, or whether it has more in common with the solid noble gases.

To address the fundamental question of whether eka-mercury is metallic in the solid state, we performed non-relativistic (NR), scalar relativistic (SR), and four-component relativistic (FR) band-structure calculations on element 112 (see *Methods*). Mercury solidifies in a rhombohedral structure that is derived from a distortion of the face-centered cubic (fcc) structure through a change in the rhombohedral angle from $\alpha = 60$ to 70°. However, zinc and cadmium both adopt hexagonal close-packed (hcp) structures. Therefore, we decided to optimize the structure of element 112 in both lattices. In the rhombohedral case, we obtained optimized lattice parameters of $a = 3.28$ Å and $\alpha = 61.5°$, and a cohesive energy of $E_{\mathrm{coh}} = 1.07$ eV from SR calculations. As the optimized structure is close to an fcc lattice, the driving force for the rhombohedral distortion with an angle of $\alpha = 70°$ in mercury does not seem to be present in element 112. The SR optimization in the hcp lattice reinforced this argument: we obtained lattice parameters of $a = 3.34$ and $c = 5.36$ Å, and a cohesive energy of $E_{\mathrm{coh}} = 1.13$ eV. A re-optimization of the lattice at the FR level of theory resulted in only slight changes in the lattice parameters ($a = 3.32$ and $c = 5.40$ Å). Thus, according to our calculations (which apply the local density approximation (LDA)), element 112 prefers the hcp lattice.

Remarkably, the calculated c/a ratios of 1.61 (SR) and 1.63 (FR) are very close to the ideal value of 1.63, unlike the c/a ratios of zinc and cadmium of 1.86 and 1.89, respectively. Thus, element 112 differs substantially from its lighter homologues on a structural level and, in this sense, more closely resembles the solid noble gases.[28] However, the cohesive energy of element 112 is slightly larger than that of mercury, but is an order of magnitude larger than those of the solid noble gases.[28] This result is consistent with the behavior of the dissociation energies of dimers of the Group 12 elements, which was investigated previously.[19] The nearest-neighbor distance in solid element 112 is calculated as 3.30 Å, substantially larger than that of 3.00 Å in rhombohedral mercury.[29]

---

[*] Prof. Dr. P. Schwerdtfeger
Center of Theoretical Chemistry and Physics
Institute of Fundamental Sciences
Massey University (Auckland Campus)
Private Bag 102904, North Shore MSC, Auckland (New Zealand)
Fax: (+64) 9-443-9779
E-mail: p.a.schwerdtfeger@massey.ac.nz

Dr. N. Gaston
Max-Planck-Institut für Physik komplexer Systeme
Nöthnitzer Strasse 38, 01187 Dresden (Germany)

Dr. I. Opahle
IFW Dresden
P.O. Box 270116, 01171 Dresden (Germany)

Prof. Dr. H. W. Gäggeler
Labor für Radio und Umweltchemie
Universität Bern, 3012 Bern (Switzerland)
and
Labor für Radio und Umweltchemie
Paul Scherrer Institut, 5232 Villigen PSI (Switzerland)

[**] This work was financed by the Royal Society of New Zealand through a Marsden Grant and by the ISAT Linkage Fund.

From the NR calculations, we obtained hcp lattice parameters of $a = 3.44$ and $c = 6.06$ Å. Thus, the NR-optimized lattice, with a c/a ratio of 1.76, is quite similar to the hcp lattices of zinc and cadmium. As expected, neglecting relativistic effects leads to a higher calculated cohesive energy of $E_{coh} = 1.66$ eV, because the valence 7s shell is more extended, allowing better mixing with the 7p shell.

The band structures corresponding to the hcp lattices optimized by NR, SR, and FR calculations are presented in Figure 1. The NR band structure (Figure 1 a) is comparable to the band structures of zinc and cadmium. Very flat 6d bands occur well below the Fermi level, and the valence 7s band crosses the Fermi level. The conduction 7p band also crosses the Fermi level near the Γ point. Thus, the system is metallic.

However, the SR band structure (Figure 1 b) is very different. The most obvious difference is the appearance of a band gap of 0.88 eV, which makes element 112 an insulator. The 6d bands overlap with the 7s bands. As the LDA applied in our calculations tends to overestimate binding energies and, therefore, to favor metallic structures, the insulating structure found here is unlikely to be a result of our choice of functional.

In addition, we calculated the band structure of the optimized rhombohedral structure, and found a slightly smaller band gap of 0.85 eV. This result is partly due to the nearest-neighbor distance of 3.28 Å, which is slightly shorter than that of 3.30 Å in the hcp structure. An NR band structure calculated for the SR-optimized geometry is very similar to the NR band structure shown in Figure 1 a, indicating that the metallicity is only weakly dependent on the lattice structure (primarily on the interatomic distances).

In the preceding discussion, spin–orbit coupling was neglected. However, as the splitting of the 7p levels into $7p_{1/2}$ and $7p_{3/2}$ states is very large for superheavy elements,[30] the lowering of the energy of the $7p_{1/2}$ conduction band is expected to reduce the size of the band gap. Thus, the possibility that element 112 is, in fact, metallic cannot be excluded on the basis of the NR and SR calculations. FR calculations are essential to determine whether element 112 is metallic. As can be seen in the FR band structure (Figure 1 c), spin–orbit coupling does indeed lead to a markedly smaller band gap of only 0.2 eV.

The SR and FR density of states (DOS) curves for the hcp structure are shown in Figure 2. The influence of the spin–orbit splitting is clearly visible: in the FR DOS curve (Figure 2 b), the $6d_{3/2}$ and $6d_{5/2}$ levels are strongly split by approximately 3.2 eV, and the $7p_{1/2}$ and $7p_{3/2}$ levels above the band gap are split by approximately 5 eV. Owing to the relativistic expansion of the 6d levels and the relativistic contraction of the 7s levels, the valence bands have predominantly 6d character, and there is significant overlap between the fully occupied 7s and 6d bands.

We conclude that element 112 is not a metal, but rather a semiconductor (under normal conditions) with a band gap of at least 0.2 eV (the result of our LDA calculations can be considered as a lower bound). As the band gap is quite small, element 112 resembles the Group 12 metals more closely than it does the noble gases.

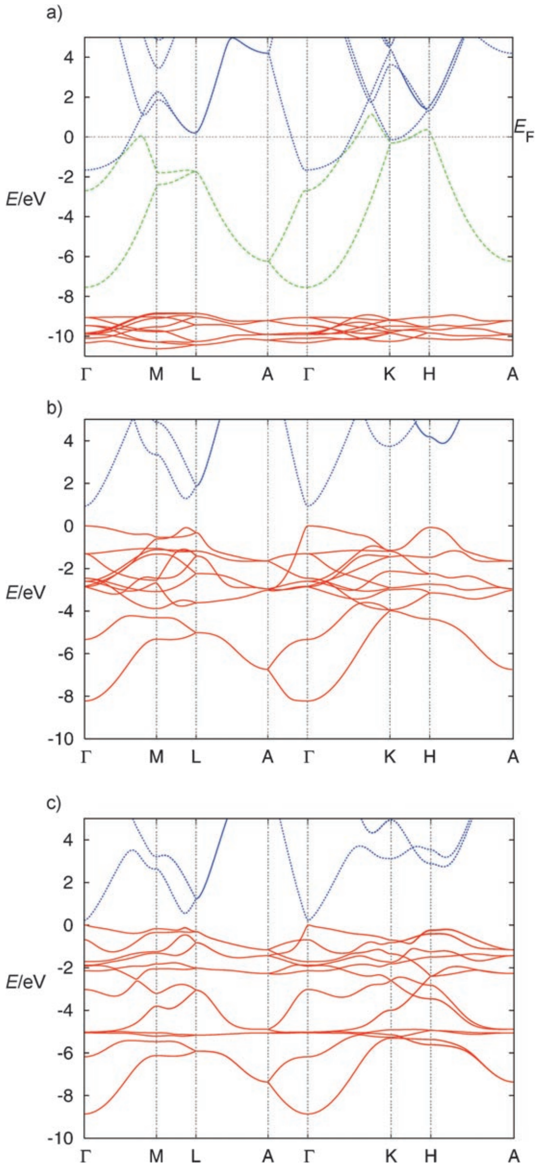

Figure 1. a) Nonrelativistic (NR), b) scalar relativistic (SR), and c) four-component relativistic (FR) band structures for the optimized hcp lattice of element 112. The p bands are represented as dotted blue lines. In (a), the d bands are represented as solid red lines, and the s bands as dashed green lines. In (b) and (c), there is considerable mixing between the s and d bands; the mixed bands are represented as solid red lines. The Fermi energy (E_F) is set to zero.

Methods

The SR and NR geometry optimizations and band-structure calculations were made using a small-core energy-consistent Stuttgart pseudopotential[25] to model the $[Xe]4f^{14}5d^{10}5f^{14}$ core.[31] Exponents smaller than 0.1 were removed from the original optimized diffuse valence basis sets, as these lead to linear dependencies and to nonconvergence of the self-consistent field (SCF) procedure. The remaining diffuse functions were re-optimized from a (8s7p5d) basis set and contracted to [7s6p4d]. The cohesive energy is counterpoise-corrected and was determined by calculating the atomic energy in the presence of basis functions placed at the positions of neighboring atoms in the solid. This correction converged with the inclusion of the first 18 neighbors. 133 k points were sampled in the irreducible part of the Brillouin zone.

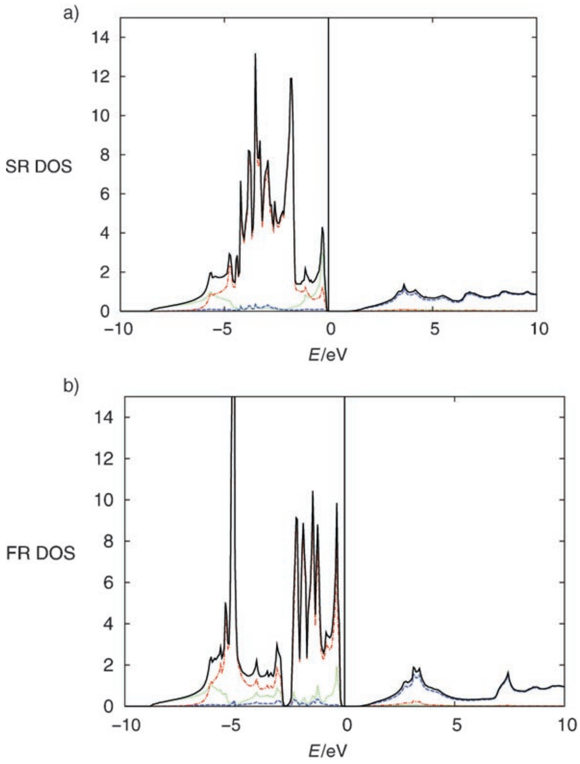

Figure 2. a) Scalar relativistic (SR), b) four-component relativistic (FR) and density of states (DOS) curves for the optimized hcp lattice of element 112. The total DOS is represented as a solid black line. The contribution of the s bands is represented as a dotted green line, that of the p bands as a dashed blue line, and that of the d bands as a dot-dashed red line. The Fermi energy is set to zero.

The LDA[32] was used because of its general suitability for metals and, in particular, the rhombohedral structure of solid mercury.[33] We also tested various other LDA and generalized gradient approximation (GGA) functionals implemented in the CRYSTAL03 code.[31] None produced band gaps smaller than those reported herein (e.g., a band gap of 1.4 eV was determined from SR calculations using the GGA functional PW91[34,35]). This observation supports our interpretation of the value determined from the LDA calculations as a lower bound.

Additionally, we performed Kohn–Sham–Dirac FR geometry optimizations and band-structure calculations to check the influence of spin–orbit coupling using the relativistic version[36] of the full-potential local orbital method[37] (RFPLO). Bloch sums of atom-like local orbitals were used as a basis set. The local orbitals were chosen as solutions to a single-particle Dirac equation in the spherically averaged crystal potential. An additional confining r^4 potential with an orbital-dependent variational parameter, which was optimized such that the total energy was minimized, was applied to the valence states.

5f, 6d, 7s and 7p states were used as the basis set. The spin–orbit-split 5f states form dispersionless bands located 63 and 69 eV below the Fermi energy. The inclusion of 5f states in the valence basis set influenced the calculated total energy only marginally (ca. 1 μHartree/atom), which justifies their neglect in the geometry optimizations with the CRYSTAL03 code. The inclusion of 6f polarization states also led to negligible changes in the band structure.

The atom-centered potentials and densities were expanded as spherical harmonic functions with a cutoff of $l_{\max} = 12$. The number of k points selected in the irreducible part of the Brillouin zone was 133. The LDA parameterization of Perdew and Wang[38] was used for the exchange-correlation potential.

The band gap determined by SR calculations using the RFPLO program (ca. 0.7 eV) was somewhat smaller than that determined from calculations using the CRYSTAL03 code (ca. 0.9 eV). This discrepancy is not due to differences in the parameterization of the LDA functional. The band gap calculated using the CRYSTAL03 code remained unchanged when the functional PW92 was used. This result indicates that the difference of 0.2 eV must be due to the different codes. A possible source for the discrepancy could be the different definitions of the SR approximation or the different basis sets used in the two codes.

Received: October 18, 2006

Keywords: density functional calculations · electronic structure · element 112 · relativistic effects · semiconductors

---

[1] *The Chemistry of Superheavy Elements* (Ed.: M. Schädel), Kluwer Academic, Dordrecht, **2003**.
[2] S. Hofmann, G. Münzenberg, *Rev. Mod. Phys.* **2000**, *72*, 733–767.
[3] Yu. Ts. Oganessian, V. K. Utyonkoy, Yu. V. Lobanov, F. Sh. Abdullin, A. N. Polyakov, I. V. Shirokovsky, Yu. S. Tsyganov, G. G. Gulbekian, S. L. Bogomolov, A. N. Mezentsev, S. Iliev, V. G. Subbotin, A. M. Sukhov, A. A. Voinov, G. V. Buklanov, K. Subotic, V. I. Zagrebaev, M. G. Itkis, J. B. Patin, K. J. Moody, J. F. Wild, M. A. Stoyer, N. J. Stoyer, D. A. Shaughnessy, J. M. Kenneally, R. W. Lougheed, *Phys. Rev. C* **2004**, *69*, 021601.
[4] Yu. Ts. Oganessian, V. K. Utyonkoy, Yu. V. Lobanov, F. Sh. Abdullin, A. N. Polyakov, I. V. Shirokovsky, Yu. S. Tsyganov, G. G. Gulbekian, S. L. Bogomolov, B. N. Gikal, A. N. Mezentsev, S. Iliev, V. G. Subbotin, A. M. Sukhov, A. A. Voinov, G. V. Buklanov, K. Subotic, V. I. Zagrebaev, M. G. Itkis, J. B. Patin, K. J. Moody, J. F. Wild, M. A. Stoyer, N. J. Stoyer, D. A. Shaughnessy, J. M. Kenneally, R. W. Lougheed, *Phys. Rev. C* **2004**, *69*, 054607.
[5] Yu. Ts. Oganessian, V. K. Utyonkov, Yu. V. Lobanov, F. Sh. Abdullin, A. N. Polyakov, R. N. Sagaidak, I. V. Shirokovsky, Yu. S. Tsyganov, A. A. Voinov, G. G. Gulbekian, S. L. Bogomolov, B. N. Gikal, A. N. Mezentsev, S. Iliev, V. G. Subbotin, A. M. Sukhov, K. Subotic, V. I. Zagrebaev, G. K. Vostokin, M. G. Itkis, K. J. Moody, J. B. Patin, D. A. Shaughnessy, M. A. Stoyer, N. J. Stoyer, P. A. Wilk, J. M. Kenneally, J. H. Landrum, J. F. Wild, R. W. Lougheed, *Phys. Rev. C* **2006**, *74*, 044602.
[6] M. Schädel, *Angew. Chem.* **2006**, *118*, 378–414; *Angew. Chem. Int. Ed.* **2006**, *45*, 368–401.
[7] Ch. E. Düllmann, W. Brüchle, R. Dressler, K. Eberhardt, B. Eichler, R. Eichler, H. W. Gäggeler, T. N. Ginter, F. Glaus, K. E. Gregorich, D. C. Hoffman, E. Jäger, D. T. Jost, U. W. Kirbach, D. M. Leek, H. Nitsche, J. B. Patin, V. Pershina, D. Piguet, Z. Qin, M. Schädel, B. Schausten, E. Schimpf, H.-J. Schött, S. Soverna, R. Sudowe, P. Thörle, S. N. Timokhin, N. Trautmann, A. Türler, A. Vahle, G. Wirth, A. B. Yakushev, P. M. Zielinski, *Nature* **2002**, *418*, 859–862.
[8] B. Fricke, *Struct. Bonding (Berlin)* **1975**, *21*, 90–145.
[9] V. Pershina in *Relativistic Electronic Structure Theory: Part 2. Applications* (Ed.: P. Schwerdtfeger), Elsevier, Amsterdam, **2004**, pp. 1–80.
[10] R. Eichler, W. Brüchle, R. Buda, S. Bürger, R. Dressler, Ch. E. Düllmann, J. Dvorak, K. Eberhardt, B. Eichler, C. M. Folden III, H. W. Gäggeler, K. E. Gregorich, F. Haenssler, D. C. Hoffman, H. Hummrich, E. Jäger, J. V. Kratz, B. Kuczewski, D. Liebe, D. Nayak, H. Nitsche, D. Piguet, Z. Qin, U. Rieth, M. Schädel, B. Schausten, E. Schimpf, A. Semchenkov, S. Soverna, R. Sudowe, N. Trautmann, P. Thörle, A. Türler, B. Wierczinski, N. Wiehl,

P. A. Wilk, G. Wirth, A. B. Yakushev, A. von Zweidorf, *Radiochim. Acta* **2006**, *94*, 181–191.

[11] R. Eichler, N. V. Aksenov, A. V. Belozerov, G. A. Bozhikov, V. I. Chepigin, R. Dressler, S. N. Dmitriev, H. W. Gäggeler, V. A. Gorshkov, F. Haenssler, M. G. Itkis, V. Ya. Lebedev, A. Laube, O. N. Malyshev, Yu. Ts. Oganessian, O. V. Petrushkin, D. Piguet, P. Rasmussen, S. V. Shishkin, A. V. Shutov, A. I. Svirikhin, E. E. Tereshatov, G. K. Vostokin, M. Wegrzecki, A. V. Yeremin, unpublished results.

[12] H. W. Gäggeler, W. Brüchle, Ch. E. Düllmann, R. Dressler, K. Eberhardt, B. Eichler, R. Eichler, C. M. Folden, T. N. Ginter, F. Glaus, K. E. Gregorich, F. Haenssler, D. C. Hoffman, E. Jäger, D. T. Jost, U. W. Kirbach, J. V. Kratz, H. Nitsche, J. B. Patin, V. Pershina, D. Piguet, Z. Qin, U. Rieth, M. Schädel, E. Schimpf, B. Schausten, S. Soverna, R. Sudowe, P. Thörle, N. Trautmann, A. Türler, A. Vahle, P. A. Wilk, G. Wirth, A. B. Yakushev, A. von Zweidorf, *Nucl. Phys. A* **2004**, *734*, 208–212.

[13] Yu. Ts. Oganessian, V. K. Utyonkov, Yu. V. Lobanov, F. Sh. Abdullin, A. N. Polyakov, I. V. Shirokovsky, Yu. S. Tsyganov, G. G. Gulbekian, S. L. Bogomolov, B. N. Gikal, S. Iliev, V. G. Subbotin, A. M. Sikhov, A. A. Voinov, G. V. Buklanov, K. Subotic, V. I. Zagrebaev, M. G. Itkis, J. B. Patin, K. J. Moody, J. F. Wild, M. A. Stoyer, N. J. Stoyer, D. A. Shaugnessy, J. M. Kennealy, P. A. Wilk, R. W. Loughreed, R. I. Il'kaeev, S. P. Vesnovskii, *Phys. Rev. C* **2004**, *70*, 064609-1-14.

[14] R. Eichler, *Radiochim. Acta* **2005**, *93*, 245–248.

[15] S. Soverna, R. Dressler, Ch. E. Düllmann, B. Eichler, R. Eichler, H. W. Gäggeler, F. Haenssler, J.-P. Niklaus, D. Piguet, Z. Qin, A. Türler, A. B. Yakushev *Radiochim. Acta* **2005**, *93*, 1–8.

[16] B. Eichler, *Kernenergie* **1976**, *19*, 307–311.

[17] N. S. Mosyagin, T. A. Isaev, A. V. Titov, *J. Chem. Phys.* **2006**, *124*, 224302.

[18] K. S. Pitzer, *J. Chem. Phys.* **1975**, *63*, 1033.

[19] J. Anton, B. Fricke, P. Schwerdtfeger, *Chem. Phys.* **2005**, *311*, 97–103.

[20] V. Pershina, T. Bastug, B. Fricke, T. Jacob, S. Varga, *Chem. Phys. Lett.* **2002**, *365*, 176–183.

[21] V. Pershina, T. Bastug, C. Sarpe-Tudoran, J. Anton, B. Fricke, *Nucl. Phys. A* **2004**, *734*, 200–203.

[22] N. W. Ashcroft, N. D. Mermin, *Solid State Physics*, Brooks-Cole, Cornell University, **1976**.

[23] J. A. Moriarty, *Phys. Lett. A* **1988**, *131*, 41–46.

[24] E. Eliav, U. Kaldor, Y. Ishikawa, *Phys. Rev. A* **1995**, *52*, 2765–2769.

[25] M. Seth, P. Schwerdtfeger, M. Dolg, *J. Chem. Phys.* **1996**, *106*, 3623–3632.

[26] P. Pyykkö, S. Riedel, M. Patzschke, *Chem. Eur. J.* **2005**, *11*, 3511–3520.

[27] C. S. Nash, *J. Phys. Chem. A* **2005**, *109*, 3493–3500.

[28] P. Schwerdtfeger, N. Gaston, R. P. Krawczyk, R. Tonner, G. E. Moyano, *Phys. Rev. B* **2006**, *73*, 064112.

[29] *CRC Handbook of Chemistry and Physics* 78th edition (Ed.:D. R. Linde), CRC, New York, **1997**.

[30] P. Schwerdtfeger, M. Seth in *The Encyclopedia of Computational Chemistry* (Eds.: P. von Ragué Schleyer, N. L. Allinger, T. Clark, J. Gasteiger, P. Kollman, H. F. Schaefer III), Wiley, New York, **1998**, pp. 2480–2499.

[31] V. R. Saunders, R. Dovesi, C. Roetti, R. Orlando, C. M. Zicovich-Wilson, N. M. Harrison, K. Doll, B. Civalleri, I. J. Bush, Ph. D'Arco, M. Llunell, CRYSTAL03, (http://www.crystal.unito.it), Turin, **2003**.

[32] S. H. Vosko, L. Wilk, M. Nusair, *Can. J. Phys.* **1980**, *58*, 1200–1211.

[33] N. Gaston, B. Paulus, K. Rosciszewski, P. Schwerdtfeger, H. Stoll, *Phys. Rev. B* **2006**, *74*, 094102.

[34] J. P. Perdew, Y. Wang, *Phys. Rev. B* **1991**, *43*, 8911–8916.

[35] J. P. Perdew, Y. Wang, *Phys. Rev. B* **1991**, *44*, 13298–13307.

[36] H. Eschrig, M. Richter, I. Opahle in *Relativistic Electronic Structure Theory: Part 2. Applications* (Ed.: P. Schwerdtfeger), Elsevier, Amsterdam, **2004**, pp. 723–776.

[37] K. Koepernik, H. Eschrig, *Phys. Rev. B* **1999**, *59*, 1743–1757; http://www.FPLO.de.

[38] J. P. Perdew, Y. Wang, *Phys. Rev. B* **1992**, *45*, 13244–13249.